Magma pressurisation sustains ongoing eruptive episode at dome-building Soufrière Hills Volcano

J. Hickey[1], K. Pascal[2,3], M. Head[1,4], J. Gottsmann[5], N. Fournier[6], S. Hreinsdottir[6], R. Syers[2]

[1] Camborne School of Mines, University of Exeter, Penryn, TR10 9FE, UK

[2] Montserrat Volcano Observatory (MVO), Flemmings, Montserrat

[3] Seismic Research Centre (SRC), University of the West Indies, Tunapuna, Trinidad and Tobago

[4] Department of Geology, University of Illinois at Urbana-Champaign, Urbana, Illinois 61801, USA

[5] School of Earth Sciences, University of Bristol, Bristol, BS8 1RL, UK

[6] GNS Science, Taupo 3384, New Zealand

ABSTRACT

Dome-building volcanoes, where long-term eruptive episodes can be interspersed with periods of intra-eruptive repose, are particularly challenging for volcanic hazard assessment. Defining the end of eruptive episodes is vitally important for the socio-economic recovery of affected communities, but highly problematic due to the potential for rapid transition from prolonged, seemingly low-risk, repose to dangerous effusive or explosive activity. It is currently unclear what constitutes the end of repose and an eruptive episode. Here we show that analysis of surface deformation can characterise repose and help define an eruptive episode. At Soufrière Hills volcano (SHV) the long-term post-2010 deformation at 12 cGPS stations requires the pressure in the magma system to increase with time; time-dependent stress relaxation or crustal creep cannot explain the deformation trends alone. Continued pressurisation within the magmatic system during repose could initiate a renewed eruption, qualifying as sustained unrest and therefore continuation of the eruptive episode. For SHV, persistent magma pressurisation highlights the need for sustained vigilance in the monitoring and management of the volcano and its surroundings, despite the last eruptive activity ending in 2010. Our results show promise for application to other dome-building volcanoes.

INTRODUCTION

Dome-building volcanoes evolve through a process of lava dome formation, with three main states: inter-eruptive repose (dormant); eruption; and intra-eruptive repose (unrest during eruptive episode) (Sheldrake et al., 2016). Eruption is mostly through effusive dome extrusion, but sudden transitions to explosive behaviour are possible (Sparks, 1997; Ogburn et al., 2015); surface deformation commonly accompanies these eruptions and the associated unrest (e.g., Sheldrake et al., 2016). A period of intra-eruptive repose classifies an eruptive episode as continuing, a consequence of the repetitive and cyclic process of dome extrusion and destruction (Sparks, 1997; Ogburn et al., 2015; Sheldrake et al., 2016; Wolpert et al., 2016). However, distinguishing intra-eruptive repose from inter-eruptive repose, through the presence or absence, respectively, of concerning geophysical or geochemical monitoring signals, is difficult (Sheldrake et al., 2016), and complicates how the end of an eruptive episode is

41 determined. Consequently, the socio-economic recovery of affected communities can be severely
42 impaired, and dome-building volcanoes are particularly challenging for hazard and risk assessment.
43
44 Volcano surface deformation is a common sign of volcanic unrest (Phillipson et al., 2013); deciphering
45 its cause is fundamental for monitoring and hazard mitigation. Magma supply (Gottsmann and Odbert,
46 2014; Odbert et al., 2014; Hickey et al., 2016) and crystallisation with volatile exsolution (Caricchi et
47 al., 2014) have been proposed as magmatic drivers of uplift, but tectonic (Bonforte et al., 2017),
48 hydrothermal (Fournier and Chardot, 2012) and viscoelastic (Segall, 2016, 2018) processes can also
49 sustain volcano deformation. The variety of different mechanisms present contrasting interpretations
50 of magma system evolution (Head et al., 2019; Pritchard et al., 2019). Deformation related solely to
51 viscoelasticity might indicate a constant or reducing pressure in the magmatic system (Head et al.,
52 2019), a decrease in eruption potential, and at dome-building volcanoes relate to inter-eruptive
53 repose. Conversely, deformation from magma supply might indicate increased eruption potential with
54 cause for concern, signifying intra-eruptive repose. Uncertainty in the cause of deformation, and
55 characterising periods of repose, is problematic and complicates eruption forecasting, hazard
56 assessment and risk mitigation (Pritchard et al., 2019).
57
58 Soufrière Hills Volcano (SHV) is an andesitic dome-building volcano in Montserrat (Figure 1) and
59 began its current eruptive episode in 1995, fed from a consistent reservoir 6 – 13 km deep (Odbert et
60 al., 2014). Eruptive activity has been intermittent (Sparks and Young, 2002; Wadge et al., 2014) with
61 periods of intra-eruptive repose generally lasting 1-2 years (Supplementary Figure 1). However, the
62 most recent eruption ended in February 2010 making the current repose period the longest yet
63 recorded. SO_2 observations at SHV since 2010 show steady emissions at an average rate of 374
64 t/day (Supplementary Figure 1), fumaroles on the lava dome maintain temperatures up to 610°C and
65 swarms of volcano-tectonic (VT) earthquakes have also been recorded (Christopher et al., 2015).
66 Continuous GPS (cGPS) measurements show island-wide inflation from 2010 onwards (Figure 1),
67 and are similar to deformation patterns commonly observed at other dome-building volcanoes
68 (Sheldrake et al., 2016). Globally, 94% of dome-building eruptive episodes last less than 20 years
69 (Wolpert et al., 2016). The current 12-year cessation of surface activity, following 15 years of
70 intermittent activity, raises the question of whether the current repose is temporary or, instead,

indicative of the end of the eruptive episode. The ambiguity is exacerbated by the presence of surface deformation whose driving processes remain unclear. The longevity of the current repose, and suggestions based on geochemical data that magma supply to SHV potentially ceased in mid-2003 (McGee et al., 2019), may indicate that non-magmatic processes (e.g., viscoelastic crustal behaviour (Segall, 2016)) are now driving the continued deformation. To assess the behaviour and evolution of the SHV magmatic system since 2010 and the nature of the current repose, we analyse the temporal deformation trends using geodetic numerical models and test the hypothesis that viscoelastic crustal behaviour is driving long-term surface inflation.

DEFORMATION MODELLING

The geodetic models used in this study incorporate a temperature-dependent viscoelastic crustal rheology, topography and 3D variations in mechanical properties (Figure 2); the methods (see Supplemental Material[1]) are easily applicable to other volcanoes by adapting volcano-specific parameters. Our model outputs are directly compared to the 2010-2018 deformation recorded at 12 cGPS sites in all 3 components (Figure 1 & Supplementary Figure 2), ensuring the widest possible model-data evaluation. The models are driven using one of four time-dependent source functions, to simulate first-order differences in the temporal evolution of the magmatic system (Figure 3). Stress-based overpressure ($\boldsymbol{\Delta P}$) and strain-based volume change ($\boldsymbol{\Delta V}$) boundary conditions are compared.

The four time-dependent source functions produce very different modelled surface displacement timeseries (Figure 3), but when compared, clear deformation patterns emerge. When the magma reservoir is in a steady state (Figure 3E), we observe minor amounts of viscoelastic creep (producing inflation) for the $\boldsymbol{\Delta P}$ models and relaxation (resulting in subsidence) for the $\boldsymbol{\Delta V}$ models. In both cases the rate-decreasing viscoelastic surface deformation becomes insignificant after ~4 years. In contrast, to produce near constant-rate continuous deformation, and/or substantial deformation over timescales greater than 4 years, requires increasing reservoir pressure or volume (Figures 3F&H). We additionally note that for elastic models their temporal surface deformation results would mirror the time-dependent source functions (Head et al., 2019).

Model results obtained with the ramp source function provide our best-fit to the observed temporal deformation trends (Figure 4). The data show increasing deformation at a near-constant rate between early-2010 and late-2018 (Figure 1), which is only achievable using the ramped source function. The resultant comparison between the normalised modelled and observed displacements shows a very close match in the temporal patterns (Figure 4A-C & Supplementary Figure 5). Some misfits do remain, particularly in the E-W components, and this is likely due to the limited distribution of GPS stations in an E-W plane due to the geography of the island, which prevents detection of peak E-W deformation magnitudes. Therefore, source geometries optimised on GPS data (like that employed in our study) are likely poor at recreating E-W surface deformation. We also do not account for sediment loading (Odbert et al., 2015). Comparisons between the absolute modelled and observed temporal displacements also show a close match (Figure 4D-F & Supplementary Figure 6) and could possibly be improved further by focussing on the spatial patterns of displacement to optimise a pressure or volume change.

MAGMA SYSTEM PRESSURISATION

Our results indicate that viscoelastic crustal deformation alone cannot explain the amplitude or temporal pattern of ongoing long-term surface deformation observed at SHV since 2010. Continued deformation over the timescales recorded in the cGPS data are only achievable when the magma reservoir is subject to an increasing pressure or volume. We compared both ΔP and ΔV source boundary conditions, with viscoelasticity producing increasing uplift (via creep) in the ΔP models, and post-uplift subsidence (via relaxation) in the ΔV models. For the thermomechanical conditions inferred beneath SHV, the choice of ΔP or ΔV is arbitrary when using our best-fit ramp source function as their viscous effects are indistinguishable on the timescales observed; they are constantly overprinted by elastic deformation from the increasing pressure or volume change (due to Boltzmann superposition (Hickey et al., 2016)), producing a near-linear temporal uplift pattern. Consequently, their normalised temporal deformation trends are broadly equal (Figure 4). The near-linear temporal dependence between all source functions and their surface deformation response is consistent and reflects the thermomechanical conditions beneath SHV. It is noted, however, that the effects of viscoelasticity produce elevated uplift for the ΔP case when compared to a purely elastic model.

The increasing magma reservoir pressure or volume at SHV since 2010 could be caused by a variety of mechanisms. The most natural driving force to assume is renewed or continued magma supply, which could initially seem in contrast to a proposed stop in magma supply in 2003 inferred from geochemical results (McGee et al., 2019). However, magma supply could still be driving this deformation if the magma supplied from a deep source region between ~2003 and present is still being stored within the shallow magmatic system and has not been erupted. A scenario of continued magma supply implies SHV may have only erupted magma supplied pre-2003 in the 2003-2010 period, which are subsequently recorded in the geochemical results (McGee et al., 2019). Continued magma supply would also be consistent with post-2003 eruptive activity and high temperature fumaroles (Christopher et al., 2015), and could be driven in part by degassing that maintains a pressure gradient between shallow magma storage and deeper magma production (Girona et al., 2015).

Alternative mechanisms to explain the inferred increasing pressure or volume relate to the role of volatiles in the magmatic system. Volatile exsolution caused by magma crystallisation (second boiling) can drive volume increases within a magma reservoir (Caricchi et al., 2014, 2021). However, it is beyond the scope of this paper to test whether a second boiling process alone can generate the necessary pressurisation to explain the observed deformation, especially in an open system emitting significant amounts of SO_2 (Christopher et al., 2015). It is also conceivable that a steady supply of volatiles, originating from a deeper source region and decoupled from the melt, is fluxing upwards through the system (Christopher et al., 2015; Caricchi et al., 2018). If the volume supplied to the shallower system is greater than the volume lost (where volatile pathways to the surface are established and sustained, accounting for the steady gas emission rates (Christopher et al., 2015)), then excess volatiles may accumulate and promote surface deformation. Alternatively, accumulation of exsolved volatiles may be driving the recorded deformation through the segregation, reorganisation and/or compaction of a transcrustal magmatic system (TCMS; Christopher et al., 2015; Cashman et al., 2017). In this scenario, volatiles could drive deformation without magma supply by buoyantly accumulating while a hot crystal mush is destabilised and reorganised. Several studies have suggested a TCMS beneath SHV (Christopher et al., 2015; Edmonds et al., 2016; Paulatto et al.,

2019), and our model source geometry could be representative of a broad, distributed network of melt storage in a TCMS (Gottsmann et al., 2020).

SUSTAINING AN ERUPTIVE EPISODE

The different magmatic processes suggested as possible causes for the surface deformation promote increases in reservoir pressure and/or volume. We cannot distinguish between pressure and volume boundary conditions for our best-fit ramp source function due to the similar temporal deformation trends they produce (Figures 3 and 4). Continued geophysical observations and additional gravity data might be able to differentiate between the suggested driving mechanisms and the pressure or volume boundary condition in the future. It is also possible that two or more of our suggested mechanisms are occurring simultaneously, with or without viscoelastic deformation. Regardless, it is clear from our results that viscoelastic crustal deformation alone cannot explain the ongoing deformation, and some component of magma system pressurisation is required. Our methods can be adapted to examine surface deformation at other dome-building volcanoes to shed further light on the nature of repose periods.

Continued magma system pressurisation at SHV implies ongoing volcanic unrest, and therefore the current repose could be classified as intra-eruptive. Despite its pressurising magmatic system, the volcano has remained in a state of repose much longer than in earlier stages of the eruptive episode. This highlights a change in magma system behaviour compared to pre-2010, and may imply that deformation observed during previous intra-eruptive periods was driven by a different mechanism. Alternatively, evolution of material properties and rheology governing the mechanical behaviour of the system (e.g., Heap et al., 2009, 2020) could mean that reservoir failure, promoting resumed eruptive activity, is now harder to achieve. More accurately identifying the nature of the mechanism(s) driving the current deformation, why it has not led to renewed eruptive activity (to date), and the role of a potential decrease in the observed deformation rate (Figure 1) requires additional and longer-term constraints and will enable improved activity forecasting and hazard assessment. However, given the solitary role of a viscoelastic crustal response can be ruled out, the continued pressurisation within the magmatic system is inconsistent with inter-eruptive repose and indicates continuing unrest with

191 potential for renewed eruptive activity. Consequently, while the most recent eruptive activity ended in
192 2010, this may not signal the end of the current eruptive episode at SHV.
193
194 [1]Supplemental Material. Supplementary methods, figures (S1-8) and table. Please visit
195 https://doi.org/10.1130/XXXX to access the supplemental material, and contact
196 editing@geosociety.org with any questions.
197
198 **ACKNOWLEDGEMENTS**
199
200 JH acknowledges a travel grant from the MVO/SRC. MH is supported by a NERC GW4+ DTP
201 studentship [NE/L002434/1] and thanks CASE partner GNS Science for extra funding. JG
202 acknowledges funding from NERC (NE/E007961/1). We thank the MVO staff for their contributions.
203
204 **REFERENCES CITED**
205
206 Bonforte, A., Fanizza, G., Greco, F., Matera, A., and Sulpizio, R., 2017, Long-term dynamics across a
207 volcanic rift: 21 years of microgravity and GPS observations on the southern flank of Mt. Etna
208 volcano: Journal of Volcanology and Geothermal Research, v. 344, p. 174–184,
209 doi:10.1016/j.jvolgeores.2017.06.005.
210 Caricchi, L., Biggs, J., Annen, C., and Ebmeier, S., 2014, The influence of cooling, crystallisation and
211 re-melting on the interpretation of geodetic signals in volcanic systems: Earth and Planetary
212 Science Letters, v. 388, p. 166–174, doi:10.1016/j.epsl.2013.12.002.
213 Caricchi, L., Sheldrake, T.E., and Blundy, J., 2018, Modulation of magmatic processes by CO2
214 flushing: Earth and Planetary Science Letters, v. 491, p. 160–171,
215 doi:10.1016/j.epsl.2018.03.042.
216 Caricchi, L., Townsend, M., Rivalta, E., and Namiki, A., 2021, The build-up and triggers of volcanic
217 eruptions: Nature Reviews Earth & Environment, doi:10.1038/s43017-021-00174-8.
218 Cashman, K. V., Sparks, R.S.J., and Blundy, J.D., 2017, Vertically extensive and unstable magmatic
219 systems: A unified view of igneous processes: Science, v. 355, doi:10.1126/science.aag3055.
220 Christopher, T.E., Blundy, J.D., Cashman, K., Cole, P., Edmonds, M., Smith, P.J., Sparks, R.S.J., and

221 Stinton, A., 2015, Crustal-scale degassing due to magma system destabilization and magma-
222 gas decoupling at Soufriere Hills Volcano, Montserrat: Geochemistry Geophysics Geosystems,
223 v. 16, p. 2797–2811, doi:10.1002/2014GC005684.Key.
224 Edmonds, M., Kohn, S.C., Hauri, E.H., Humphreys, M.C.S., and Cassidy, M., 2016, Extensive, water-
225 rich magma reservoir beneath southern Montserrat: Lithos, v. 252–253, p. 216–233,
226 doi:10.1016/j.lithos.2016.02.026.
227 Fournier, N., and Chardot, L., 2012, Understanding volcano hydrothermal unrest from geodetic
228 observations: Insights from numerical modeling and application to White Island volcano, New
229 Zealand: Journal of Geophysical Research: Solid Earth, v. 117, p. 1–16,
230 doi:10.1029/2012JB009469.
231 Girona, T., Costa, F., and Schubert, G., 2015, Degassing during quiescence as a trigger of magma
232 ascent and volcanic eruptions: Scientific Reports, v. 5, p. 1–7, doi:10.1038/srep18212.
233 Gottsmann, J., Flynn, M., and Hickey, J., 2020, The Transcrustal Magma Reservoir Beneath Soufrière
234 Hills Volcano, Montserrat: Insights From 3-D Geodetic Inversions: Geophysical Research
235 Letters, v. 47, doi:10.1029/2020gl089239.
236 Gottsmann, J., and Odbert, H., 2014, The effects of thermomechanical heterogeneities in island arc
237 crust on time-dependent preeruptive stresses and the failure of an andesitic reservoir: Journal of
238 Geophysical Research: Solid Earth, v. 119, p. 4626–4639, doi:10.1002/2014JB011079.
239 Head, M., Hickey, J., Gottsmann, J., and Fournier, N., 2019, The Influence of Viscoelastic Crustal
240 Rheologies on Volcanic Ground Deformation: Insights From Models of Pressure and Volume
241 Change: Journal of Geophysical Research: Solid Earth, doi:10.1029/2019jb017832.
242 Heap, M.J., Villeneuve, M., Albino, F., Farquharson, J.I., Brothelande, E., Amelung, F., Got, J.L., and
243 Baud, P., 2020, Towards more realistic values of elastic moduli for volcano modelling: Journal of
244 Volcanology and Geothermal Research, v. 390, doi:10.1016/j.jvolgeores.2019.106684.
245 Heap, M.J., Vinciguerra, S., and Meredith, P.G., 2009, The evolution of elastic moduli with increasing
246 crack damage during cyclic stressing of a basalt from Mt. Etna volcano: Tectonophysics, v. 471,
247 p. 153–160, doi:10.1016/j.tecto.2008.10.004.
248 Hickey, J., Gottsmann, J., Nakamichi, H., and Iguchi, M., 2016, Thermomechanical controls on
249 magma supply and volcanic deformation: application to Aira caldera, Japan: Scientific Reports,
250 v. 6, p. 32691, doi:10.1038/srep32691.

McGee, L., Reagan, M., Handley, H., Turner, S., Sparks, R.S., Berlo, K., Barclay, J., and Turner, M., 2019, Volatile behaviour in the 1995-2010 eruption of the Soufrière Hills Volcano, Montserrat recorded by U-series disequilibria in mafic enclaves and andesite host: Earth and Planetary Science Letters, v. 524, p. 115730, doi:10.1016/j.epsl.2019.115730.

Odbert, H.M., Ryan, G. a., Mattioli, G.S., Hautmann, S., Gottsmann, J., Fournier, N., and Herd, R. a., 2014, Volcano geodesy at the Soufriere Hills Volcano, Montserrat: a review: Geological Society, London, Memoirs, v. 39, p. 195–217, doi:10.1144/M39.11.

Odbert, H., Taisne, B., and Gottsmann, J., 2015, Deposit loading and its effect on co-eruptive volcano deformation: Earth and Planetary Science Letters, v. 413, p. 186–196, doi:10.1016/j.epsl.2015.01.005.

Ogburn, S.E., Loughlin, S.C., and Calder, E.S., 2015, The association of lava dome growth with major explosive activity (VEI ≥ 4): DomeHaz, a global dataset: Bulletin of Volcanology, v. 77, doi:10.1007/s00445-015-0919-x.

Paulatto, M., Moorkamp, M., Hautmann, S., Hooft, E., Morgan, J. V., and Sparks, R.S.J., 2019, Vertically Extensive Magma Reservoir Revealed From Joint Inversion and Quantitative Interpretation of Seismic and Gravity Data: Journal of Geophysical Research: Solid Earth, v. 124, p. 11170–11191, doi:10.1029/2019JB018476.

Phillipson, G., Sobradelo, R., and Gottsmann, J., 2013, Global volcanic unrest in the 21st century: An analysis of the first decade: Journal of Volcanology and Geothermal Research, v. 264, p. 183–196, doi:10.1016/j.jvolgeores.2013.08.004.

Pritchard, M.E., Mather, T.A., McNutt, S.R., Delgado, F.J., and Reath, K., 2019, Thoughts on the criteria to determine the origin of volcanic unrest as magmatic or non-magmatic: Philosophical Transactions of the Royal Society A: Mathematical, Physical and Engineering Sciences, v. 377, doi:10.1098/rsta.2018.0008.

Segall, P., 2018, Magma chambers: What we can, and cannot, learn from volcano geodesy: Philosophical Transactions of the Royal Society A: Mathematical, Physical and Engineering Sciences, v. 377, doi:10.1098/rsta.2018.0158.

Segall, P., 2016, Repressurization following eruption from a magma chamber with a viscoelastic aureole: Journal of Geophysical Research: Solid Earth, v. 121, p. 8501–8522, doi:10.1002/2016JB013597.

Sheldrake, T.E., Sparks, R.S.J., Cashman, K. V., Wadge, G., and Aspinall, W.P., 2016, Similarities and differences in the historical records of lava dome-building volcanoes: Implications for understanding magmatic processes and eruption forecasting: Earth-Science Reviews, v. 160, p. 240–263, doi:10.1016/j.earscirev.2016.07.013.

Sparks, R.S.J., 1997, Causes and consequences of pressurisation in lava dome eruptions: Earth and Planetary Science Letters, v. 150, p. 177–189, doi:10.1016/s0012-821x(97)00109-x.

Sparks, R.S.J., and Young, S.R., 2002, The eruption of Soufriere Hills Volcano, Montserrat (1995-1999): overview of scientific results: Geological Society, London, Memoirs, v. 21, p. 45–69, doi:10.1144/GSL.MEM.2002.021.01.03.

Wadge, G., Voight, B., Sparks, R.S.J., Cole, P.D., Loughlin, S.C., and Robertson, R.E.A., 2014, An overview of the eruption of Soufrière Hills Volcano, Montserrat from 2000 to 2010: Geological Society, London, Memoirs, v. 39, p. 1–39, doi:10.1144/M39.1.

Wolpert, R.L., Ogburn, S.E., and Calder, E.S., 2016, The longevity of lava dome eruptions: Journal of Geophysical Research: Solid Earth, v. 121, p. 676–686, doi:10.1002/2015JB012435.

FIGURE CAPTIONS

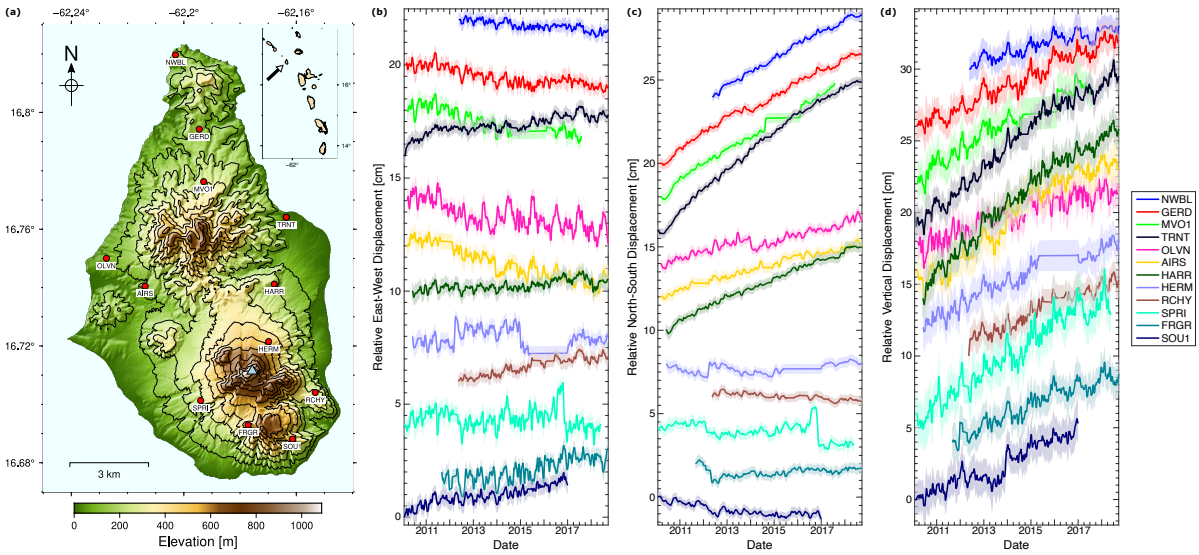

Figure 1: *cGPS network and recorded deformation. (A) DEM of Montserrat showing cGPS stations (red circles) and active vent (blue triangle). Inset map shows the Eastern Caribbean with Montserrat indicated by the arrow. (B) Relative east-west deformation with time for the cGPS stations shown in A.*

Time series are offset in the y-axis for added clarity; shaded bars are 95% confidence bounds. (C) Same as B but for north-south deformation (D) Same as B but for vertical deformation.

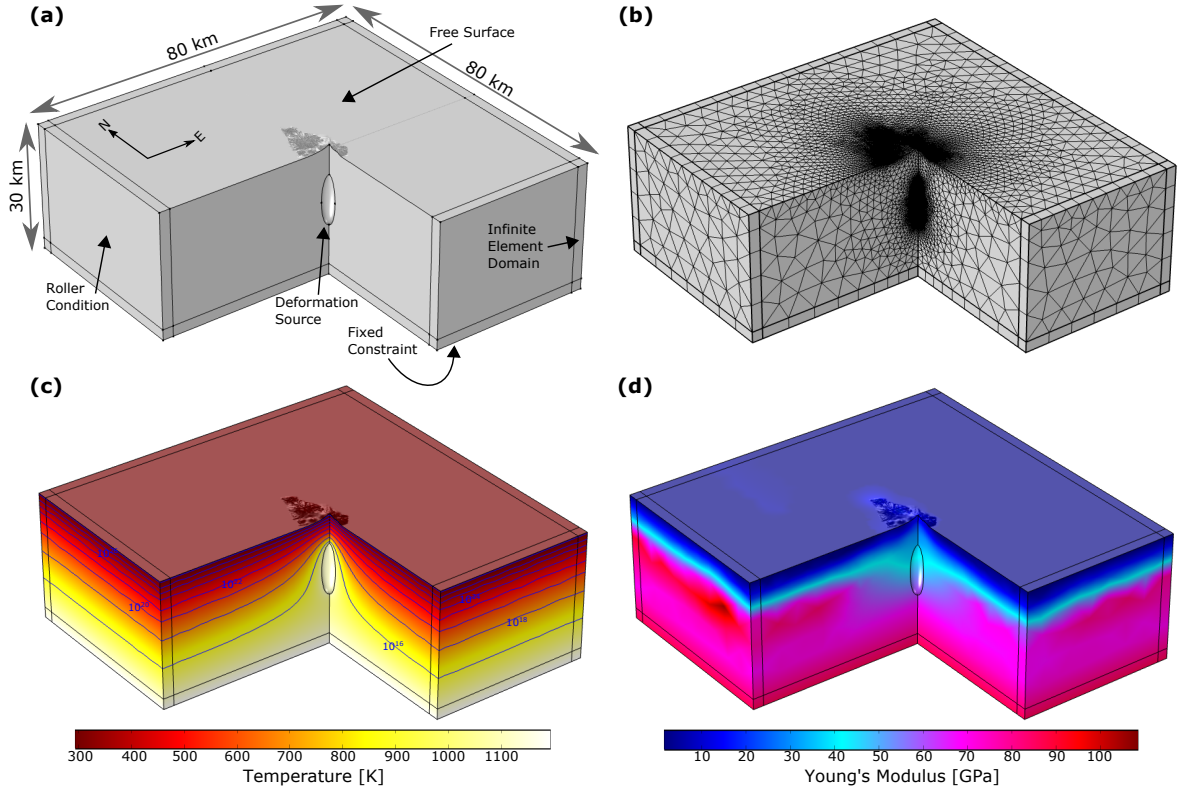

Figure 2: *Finite Element Analysis model. (A) Geometry and boundary conditions. (B) Meshed geometry. (C) Modelled steady-state temperature distribution; contours indicate viscosity used in the viscoelastic models. (D) Three-dimensional distribution of static Young's Modulus.*

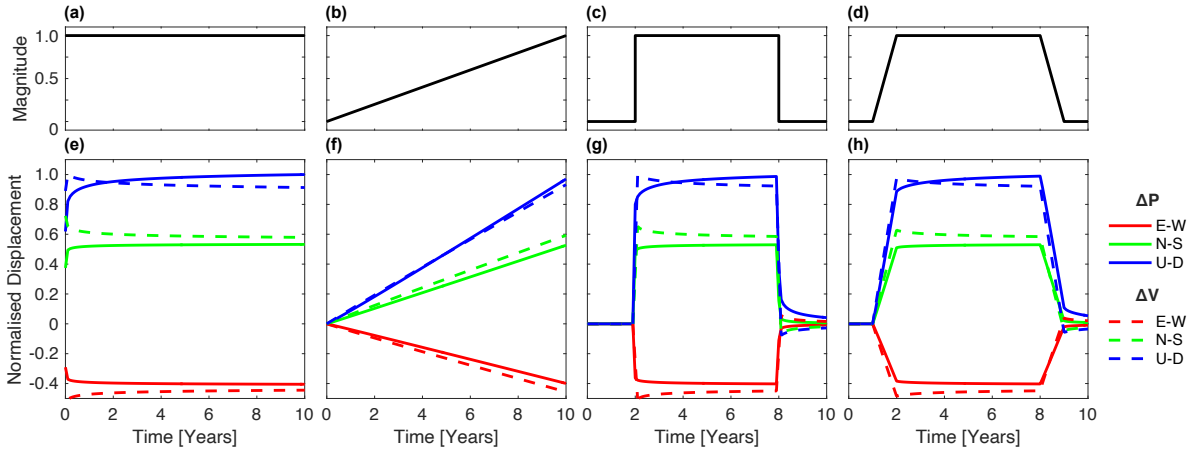

Figure 3: *Model source functions and results. (A-D) Temporal functions applied to the deformation source boundary conditions: static (A), ramp (B), instant pulse (C), and gradual pulse (D). (E-H)*

Normalized displacement timeseries for the AIRS cGPS site for the four temporal functions: static (E), ramp (F), instant pulse (G), and gradual pulse (H). Solid and dashed lines represent the ***Δ***P *and* ***Δ***V *boundary conditions, respectively; colours differentiate the 3 components of deformation (red: east-west, green: north-south, blue: vertical). Results are normalized to the maximum deformation across the 3 components and across the 4 model functions (in this case vertical and static). The same temporal trends are seen in other cGPS site locations (Supplementary Figures 3 & 4).*

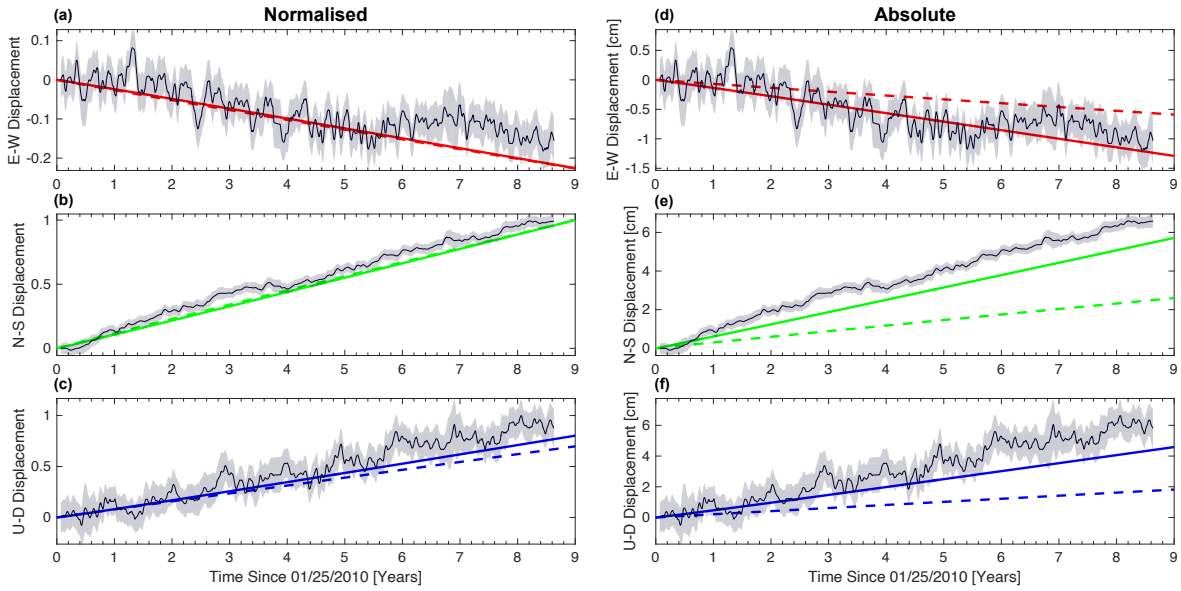

Figure 4: *Normalised and absolute model-data comparison for cGPS site GERD and the ramp temporal source function. (A-C) Normalised surface displacements for the east-west (A), north-south (B) and vertical (C) components, where the thin black line and shaded grey region display the recorded deformation and error bounds, and the solid and dashed coloured lines show the model results for a* ***Δ***P *and* ***Δ***V *boundary condition, respectively. Model and data are normalized to the maximum absolute deformation across the 3 components (in this case vertical). (D-F) Same as A-C but the model and data have not been normalized.*